ARTICLE

Measurement of Photoionization Cross Sections of the Excited States of Titanium†

Jia-jun Yang, Xing-yong Hu, Hong-xia Wu, Jian-mei Fan, Ran Cong, Yi Cheng, Xue-han Ji, Guan-xin Yao, Xian-feng Zheng*, Zhi-feng Cui

Institute of Atomic and Molecular Physics, Anhui Normal University, Wuhu 241000, China

(Dated: Received on August 21, 2009; Accepted on September 27, 2009)

Resonance-enhanced multiphoton ionization of the titanium atoms has been investigated in the 293–321 nm wavelength. We couple a laser-ablated metal target into a molecular beam to produce free atoms. Ions produced from photoionization of the neutral atoms are monitored by a home-built time-of-flight mass spectrometer. Photoionization cross sections of the excited states of Ti *I* were deduced from the dependence of the ion signal intensity on the laser intensity for photon energies close to the ionization threshold. The values obtained range from 0.2 Mb to 6.0 Mb. No significant isotope-dependence was found from measurements of the photoionization cross sections of ^{46}Ti, ^{47}Ti, and ^{48}Ti.

Key words: Photoionization cross section, Excited state, Titanium

I. INTRODUCTION

Excited-state photoionization is important to understanding hot stellar atmospheres, controlled thermonuclear research (CTR) plasmas, and radiative recombination [1]. State-specific research on the photoionization of atoms and molecules has flourished in recent years due to the development of intense, tunable, narrowband lasers. Rothe has pioneered studies of photoionization cross sections in the excited states of lithium and sodium using radiative electron-ion recombination and shocked-heated plasmas [2]. The photoionization cross section of the lithium 2p state was deduced from absolute intensity measurements. The atomic beam and the laser saturation technique enabled measurements of the photoionization cross sections of excited alkali atoms [3–11] and of alkaline-earth metal atoms [12–14]. Baig *et al.* have recently reported photoionization cross sections (above the first ionization threshold) of excited states that include the 2p, 3d, and 3s states of lithium [8], the 4s and 4d states of sodium [9,10], the 4p, 5d, 7s states of potassium [11], and the 3s3p state of magnesium using a pump-probe scheme [14].

In contrast to the aforementioned photoionization studies, few experimental and theoretical studies have focused on 3d metal atoms to date. In terms of experimental considerations, such studies have been limited due to the high melting point and low vapor pressures of transition metals. Theoretical studies have been hindered by the enormous number of ionization channels. Early studies of the resonant ionization of excited atoms have been summarized by Saloman, and calculations have been presented for several excited states at the Hartree-Fock level of theory using the relativistic corrections of Cowan [15–18]. Gobert *et al.* measured photoionization cross sections of the excited states of Fe, Co, Ti, Ni, and Cr atoms using Ar^+ beam sputtering of the different metal samples in ultrahigh vacuum followed by two-step, one-color ionization [19]. The reported cross sections for several excited states in the UV region were on the order of 10 Mb. There has been widespread disagreement regarding the measured values of these cross sections and there exists inconsistency between the experiments and the calculations. For example, identical experimental characterizations of the $y^3D_3^\circ$ state of Ni have suggested cross sections of 7 Mb according to Gobert [19] and 0.35 Mb as published by Saloman [16]. For the $w^3F_3^\circ$ state of Ti, the measured value was 30 Mb [19], but a value of 1.3 Mb was calculated using quantum-defect theory [19]. Therefore, there is a need for additional experimental measurements of photoionization cross sections to better understand the excited states of 3d metals.

In the present work, we extend our previous studies on photoionization cross sections of the excited states of Ti *I*, Co *I*, and Ni *I* [20] and obtain new data of photoionization of the excited atomic states of titanium. Atoms are produced using a method that improves upon earlier techniques such as high temperature vaporization or sputtering with an Ar^+ beam. We couple a laser-ablated metal target into a molecular beam to produce a pulsed atomic beam. Measurements on atoms produced in this way are more accurate due to the high beam strength, low-energy initial population, and negligible

†Part of the special issue for "the Chinese Chemical Society's 11th National Chemical Dynamics Symposium"

*Author to whom correspondence should be addressed. E-mail: zxf7002@mail.ahnu.edu.cn

collisional quenching of the excited states. Photoionized atoms are monitored by a time-of-flight (TOF) mass spectrometer. Photoionization cross sections of the excited states are deduced from the ionization signal intensity as a function of the laser intensity.

II. EXPERIMENTS

We performed the experiments using a conventional molecular beam TOF mass spectrometer [20–22]. The experimental arrangement is shown in Fig.1. The base pressure of the instrument was maintained at 133 mPa, the pressure of the source chamber with the pulsed valve running was <1 mPa, and the ionization chamber was held at 0.1 mPa. The titanium atoms produced from laser ablation of the metal sample, which was fixed to the rotary axis of a step motor, were carried by an argon beam pulsed out of a valve (General Valve, Series 9). The seeded argon beam was collimated to 2.8 cm downstream by a 1-mm diameter skimmer into the ionization chamber. The ultraviolet (UV) laser radiation was focused by a lens (f=30 cm) into the photoionization zone where it was crossed with the atomic beam. Ions generated by multiphoton ionization (MPI) processes were monitored by a TOF mass spectrometer. The ion-current signals output from the microchannel plates (MCP) were transmitted to a 400 MHz digital oscilloscope (Tektronix, TDS460A), where they were averaged and transferred to a computer via an RS232 interface. In the spectroscopic scan, the ion-current signals from the mass spectrometer were fed into a Boxcar averager (SR250) and sampled using an automatic data acquisition system. The spectra were recorded by scanning a visible dye laser at a rate of 0.004 nm/s. This corresponded to a UV scan rate of 0.002 nm/s.

The ablation laser radiation is the second harmonic (532 nm) of a Q-switched Nd:YAG laser (Spectra-Physics, 10 ns). The laser beam was focused onto the surface of the sample. The laser energy required for saturation in the resonant step was determined by the applied ablation laser energy. The ablation laser energy dictated the number density of atoms in the initial state, higher ablation laser energies required more excitation laser energy to saturate the resonant transition. Therefore, in this experiment the ablation laser energy was set as low as possible.

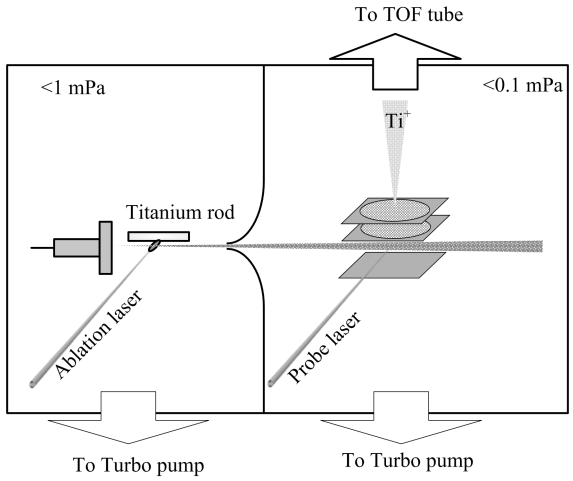

FIG. 1 Schematic of the experimental setup used for the photoionization study of the excited states of the titanium atoms.

The excitation and ionization source was a dye laser (Sirah) pumped by the second harmonic (532 nm) of a Q-switched Nd:YAG laser (Spectra-Physics, 10 ns). The required wavelength range of 293–321 nm was obtained by frequency-doubling the output of the dye laser (R590, DCM) using a KDP crystal. The laser wavelength was monitored by a wavemeter (Burleigh WA-4500) with an accuracy of 0.01 cm^{-1}. The laser bandwidth was about 0.1 cm^{-1} and the duration of the laser pulse, τ_L, was 10 ns. The **E** vector of the linearly polarized UV radiation was parallel to the TOF tube.

The photoion yields were measured as a function of the ionization laser energy. In this work, a series of identical-transmission meshes were used to vary the probe laser energy. Pulse energies were measured before the laser beam hit the first mesh using a power meter (PE10BB, OPHIR) and pulse energies after the meshes were calculated from the mesh transmission data. For each energy value, E_L, at a resonant wavelength, the associated TOF peak profile was averaged over 300 laser shots. The peak areas were obtained through integrating a Gaussian curve resulting from fitting the experimental TOF profile with the software PeakFit (Jandel Scientific).

The titanium rod sample (99.7%) was purchased from Alfa Aesar (USA) and used without further processing.

III. RESULTS AND DISCUSSION

In order to measure photoionization cross sections from excited states with short lifetimes of less than the pulse width, we must not ignore spontaneous decay of the excited state during the laser pulse period. It has been suggested that this spontaneous decay can cause the number density of excited atoms to decrease exponentially [23]. However, the loss of atoms from the short-lived excited state is partially compensated by further excitation of atoms from the ground state in order to maintain transition saturation. Because atoms entering the probing zone are free from collisions under the supersonic atomic beam, collisional quenching of the excited state may be ignored. Furthermore, since the transition was saturated throughout the pulse and the laser was linearly polarized (ΔM=0) [6] during the laser pulse.

$$N_1(t) = N_2(t) = \frac{N_T(t)}{2} \quad (1)$$

DOI:10.1088/1674-0068/22/06/615-620

where $N_1(t)$ and $N_2(t)$ indicate the number densities of atoms in the initial state and in the excited state at time t, respectively, and $N_T(t)$ is the sum. The loss rate due to ionization from the resonant state is given by

$$\frac{\mathrm{d}N_T(t)}{\mathrm{d}t} = -\frac{I(t)\sigma}{h\nu}N_2(t) = -\frac{I(t)\sigma}{2h\nu}N_T(t) \tag{2}$$

here $I(t)$ is the time-dependent intensity at a certain laser wavelength and σ is the photoionization cross section of the intermediate resonant state in the context of all accessible continuum states at this wavelength. Integration of Eq.(2) yields

$$N_T(t) = N_0 \cdot \exp\left[-\frac{\sigma}{2h\nu}\int_0^t I(t')\mathrm{d}t'\right] \tag{3}$$

where N_0=N_T (t=0). During the laser pulse period, τ, the total ion number density is given by

$$\begin{aligned} N=&\int_0^\tau \frac{I(\tau)\cdot\sigma}{h\nu}N_2(\tau)\mathrm{d}t \\ =&N_0\left\{\int_0^\tau \exp\left[-\frac{\sigma}{2h\nu}\int_0^\tau I(\tau')\mathrm{d}\tau'\right]\right. \\ &\left.\mathrm{d}\left[-\frac{\sigma}{2h\nu}\int_0^\tau I(\tau')\mathrm{d}\tau'\right]\right\} \end{aligned} \tag{4}$$

$$\int_0^\tau I(\tau)\mathrm{d}\tau = \frac{E}{A} \tag{5}$$

where E is the laser pulse energy and A is the cross-sectional area of the laser beam and of the atomic beam. Integrating Eq.(4) yields

$$N = N_0\left[1-\exp\left(-\frac{\sigma\cdot E}{2h\nu A}\right)\right] \tag{6}$$

In this experiment, the strength of the extraction electric field, the strength of the acceleration field, and the MCP driven voltage in the time-of-flight mass spectrometer were kept constant. Therefore, the intensity of the ion current signal is proportional to the total number of ions N produced during the pulse and

$$S = \kappa N = \kappa N_0\left[1-\exp\left(-\frac{\sigma\cdot E}{2h\nu A}\right)\right] \tag{7}$$

This experiment measures the pulse energy E and the cross-sectional area A as used in Eq.(7). The photoionization cross section σ was extracted from a least-squares fit to the experimental data of S as a function of E/A. The error in this method primarily derives from (i) determining the cross-sectional area with an energy distribution, (ii) measuring the pulse energy due to the energy meter (±5%) and the mesh transmission (±10%), and (iii) the statistical measurement (±10%). Before using the UV radiation, the stronger part of the laser beam was chosen with the help of an iris and a UV lens and thus a uniform spatial distribution of the focused laser beam at the probe zone was realized. The cross-sectional area was measured at the atom-beam pass using Kodak film. The burn spot of the film was enlarged 20 times with a microscope (JC-10, China) to deduce the cross-sectional area. The diameter of the burn spot was found to be 400 μm at the laser wavelength of 300 nm. The uncertainty from the determination of the cross-sectional area is estimated to be less than 20%. The spontaneous decay can cause the number density of excited atoms to decrease during the laser pulse. When the radiation trapping process exists, the transition probability A_{ij} change to an apparent value $A_{ij}{}^{\mathrm{eff}}$=γA_{ij}, $0\leq\gamma\leq1$ [24]. The radiation trapping might reduce the decay of the excited state from the spontaneous radiation. However, in the context of a high photon flux and a large absorption cross section of a resonance transition, the dynamic equilibrium in the populations of the short-life excited state and the lower-lying state could be maintained throughout the laser pulse. Therefore the error contribution due to the decay of the short-life excited state should be trivial. In the earlier work on the measurement of the absolute photoionization cross sections of the short-life excited states by Dunning *et al.*, the correction for this decay is proposed to be ±10% [23]. The overall root-mean-square error in the determination of the absolute photoionization cross sections is ∼27%.

A typical TOF mass spectrum as a result of (1+1) resonance enhanced multiphoton ionization of Ti *I* is shown in Fig.2. Both TOF mass spectra were obtained at a laser energy of 2 mJ/pulse. It is evident that the off-resonant signal was rather weak and was less than 10% intensity of the resonant signal. At resonance, ionization via a direct two-photon process is negligible relative to ionization via the intermediate state, which ensures the accurate assessment of the extracted cross sections. We observe from Fig.2 that five isotopes, ^{46}Ti, ^{47}Ti, ^{48}Ti, ^{49}Ti, and ^{50}Ti, were well-separated in time. This observation allows us to measure the photoionization cross section of isotopes under the same experimental conditions. The relative intensities were consistent

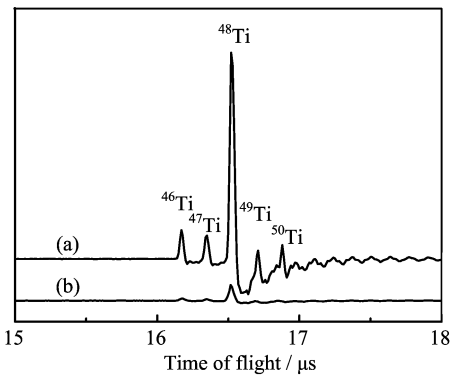

FIG. 2 Multiphoton ionization TOF mass spectra of Ti (a) at the resonant wavelength of 316.008 nm and (b) at the off-resonant wavelength of 316.018 nm.

DOI:10.1088/1674-0068/22/06/615-620

TABLE I Photoionization cross sections from the excited states in titanium.

Wavelength/nm	Lower state	Upper state	σ/Mb
293.356	$3d^24s^2$ (a^3F_2)	$3d^24s4p$ ($v^3F^\circ_3$)	0.63, 0.80[a]
293.733	$3d^24s^2$ (a^3F_3)	$3d^24s4p$ ($v^3F^\circ_4$)	0.96, 1.20[a]
294.195	$3d^24s^2$ (a^3F_2)	$3d^24s4p$ ($v^3F^\circ_2$)	0.44, 0.76[a], 0.64[a]
317.943	$3d^24s^2$ (a^3F_4)	$3d^24s4p$ ($z^3H^\circ_4$)	1.55, 1.43(^{47}Ti), 1.40 (^{46}Ti)
315.764	$3d^24s^2$ (a^3F_3)	$3d^24s4p$ ($z^3H^\circ_4$)	1.95, 1.82 (^{47}Ti), 1.75 (^{46}Ti)
317.095	$3d^24s^2$ (a^3F_4)	$3d^24s4p$ ($z^3H^\circ_5$)	5.35, 5.60 (^{47}Ti), 5.42 (^{46}Ti)
315.109	$3d^24s^2$ (a^3F_2)	$3d^24s4p$ ($y^3P^\circ_1$)	2.97, 2.95 (^{47}Ti), 3.10 (^{46}Ti)
316.008	$3d^24s^2$ (a^3F_3)	$3d^24s4p$ ($y^3P^\circ_2$)	1.38, 1.22 (^{47}Ti), 1.32 (^{46}Ti)

[a] Calculations using Hartree-Fock code [16,18].

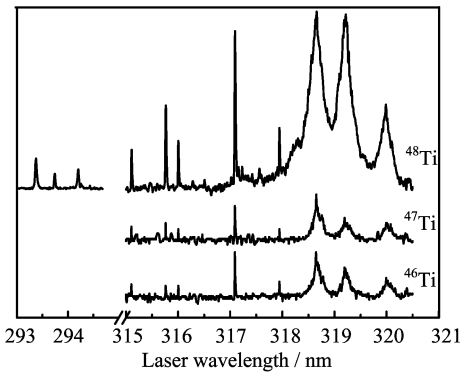

FIG. 3 Multiphoton ionization spectra of the titanium isotopes.

with the natural abundance ratio (11:10:100:7:7) [25]. The strongest signal corresponded to the dominant isotope ^{48}Ti. Due to interference from the strongest peak of ^{48}Ti, the signal-to-noise ratios for ^{49}Ti and ^{50}Ti were insufficient to evaluate the signal intensity and further to derive the absolute photoionization cross sections.

The multiphoton ionization spectra of Ti *I* shown in Fig.3, was obtained by scanning the dye laser wavelength. Resonances involved in the measurement were assigned [26,27] and labels for the initial and intermediate levels are listed in Table I. These resonances were confirmed to be (1+1) resonant ionization. Since the initially excited atoms will cool to their lower electronic states during their propagation into the ionization zone, these resonances correspond to transitions from the lower electronic states: $a^3F_{2,3,4}$ of Ti *I*. In Fig.3, the spectra were obtained from two independent experiments, one ranging from 293 nm to 295 nm and the other ranging from 315 nm to 321 nm. Within each wavelength range, the relative intensity is correct and thus indicates the contribution of the number density in the initial state and the photoionization cross section of the resonant state. In the wavelength region of 318–321 nm, three very broad resonances were observed. The full width of half maximum is about 6.4, 6.4, and 3.3 cm^{-1} respectively corresponding to the resonance at 318.657, 319.223, and 319.990 nm. Our experiment has confirmed that each of the three resonances belongs to a two photon process. The ion-forming mechanism might be involved in the autoionization due to many ionization channels existing above the ionization threshold for the many-electron 3d-metal atom. In addition, the REMPI spectra of ^{46}Ti and ^{47}Ti were investigated in the 315–321 nm region. In the present measurement, only a few sharp and narrow resonant lines were chosen to study the photoionization process.

The signal intensity has been measured as a function of the laser intensity, E/A, in resonance in the context of $v^3F^\circ_2 \leftarrow a^3F_2$, $v^3F^\circ_3 \leftarrow a^3F_2$, $v^3F^\circ_4 \leftarrow a^3F_3$, $z^3H^\circ_4 \leftarrow a^3F_4$, $z^3H^\circ_4 \leftarrow a^3F_3$, $z^3H^\circ_5 \leftarrow a^3F_4$, $y^3P^\circ_1 \leftarrow a^3F_2$, and $y^3P^\circ_2 \leftarrow a^3F_3$ transitions. Typical data for the photoionization of $z^3H^\circ_4$, $z^3H^\circ_5$, $y^3P^\circ_1$, and $y^3P^\circ_2$ are shown in Fig.4 and Fig.5. It is clear that the signal intensity is linearly dependent on the laser energy at low energies, which indicates that the resonant step may be saturated. At the higher laser intensities, the ion signal shows a saturation trend, which is to be expected from Eq.(7). A fit of the experimental data obtained in the context of $z^3H^\circ_4 \leftarrow a^3F_4$, $z^3H^\circ_4 \leftarrow a^3F_3$, and $z^3H^\circ_5 \leftarrow a^3F_4$ consistent with Eq.(6) leads to σ=1.55, 1.95, and 5.35 Mb, respectively. For $y^3P^\circ_1$ and $y^3P^\circ_2$ states, the photoionization cross sections obtained from the fit are 2.97 and 1.38 Mb, respectively. For the $v^3F^\circ_2$, $v^3F^\circ_3$, and $v^3F^\circ{}_4$ states, the photoionization cross sections are 0.44, 0.63, and 0.96 Mb, respectively and these values are in agreement with Hartree-Fock calculations that include relativistic corrections and an empirical adjustment of the calculated energies to fit the observed spectrum of Ti [18]. This agreement indicates that the present method is suitable for measuring photoionization cross sections of 3d-metal atoms.

The stable isotopes ^{46}Ti, ^{47}Ti, ^{49}Ti, and ^{50}Ti were recorded in the TOF mass spectrum along with ^{48}Ti. However, as displayed in Fig.2, the signal-to-noise ratio of ^{49}Ti and ^{50}Ti was insufficient to derive the signal intensity and obtain reliable cross section data. The experimental and fitted curves for the $z^3H^\circ_4$, $z^3H^\circ_4$, $y^3P^\circ_1$, and $y^3P^\circ_2$ states of ^{46}Ti and ^{47}Ti are also shown in Fig.4

DOI:10.1088/1674-0068/22/06/615-620

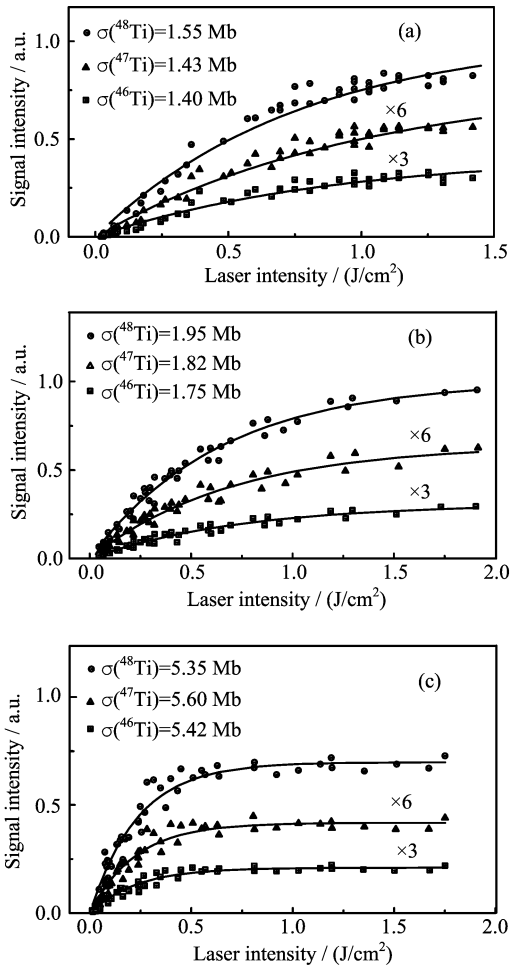

FIG. 4 Photoionization data for the $3d^24s4p$ level of the Ti atoms corresponding to (a) $z^3H_4^\circ \leftarrow a^3F_4$ with the wavelength of 317.943 nm, (b) $z^3H_4^\circ \leftarrow a^3F_3$ with the wavelength of 315.764 nm, and (c) $z^3H_5^\circ \leftarrow a^3F_4$ transitions with the wavelength of 317.095 nm. The solid lines are the least-squares fits to Eq.(6) that were used to extract photoionization cross sections.

and Fig.5, where the curves were scaled by a factor of 6 for ^{47}Ti and by a factor of 3 for ^{46}Ti. Given the experimental uncertainty of 27%, no significant cross-sectional differences could be observed for ^{46}Ti, ^{47}Ti, and ^{48}Ti.

The photoionization cross section data obtained in this work are reported alongside values from calculations in Table I. The photoionization cross sections for the $y^3P_2^\circ$ state via the $y^3P_2^\circ \leftarrow a^3F_3$ transition and the $z^3H_4^\circ$ via the $z^3H_4^\circ \leftarrow a^3F_4$, transition are reported for the first time.

IV. CONCLUSION

In this work, a TOF mass spectrometer coupled with a pulsed atomic beam is used to measure photoionization cross sections. The absolute photoionization cross sections of the excited states of Ti I are measured for photon energies close to the ionization threshold. The overall uncertainty is estimated to be less than 27%, which can be attributed to errors in the measurement of the cross-sectional area of the laser beam and to measurements of laser energy. In addition, the photoionization cross sections of the Ti isotopes were determined and were found to be identical within the investigated ionization region.

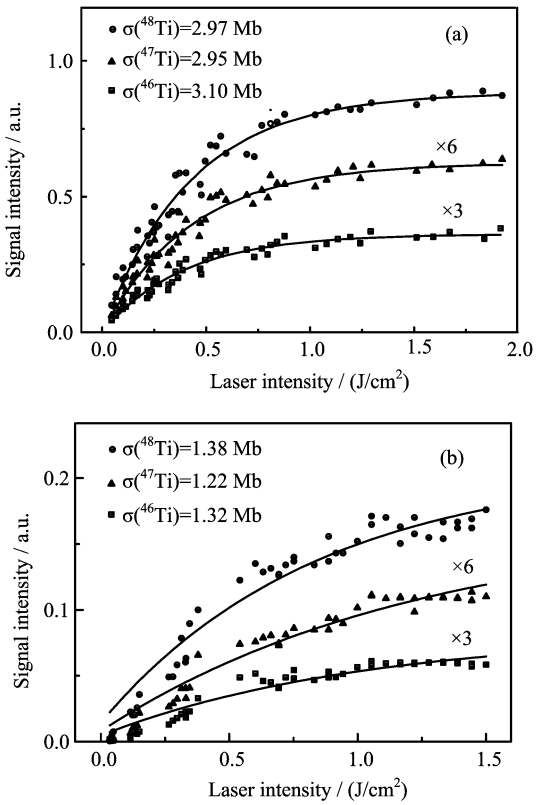

FIG. 5 Photoionization data for the $3d^24s4p$ level of the Ti atoms corresponding to (a) $y^3P_1^\circ \leftarrow a^3F_2$ with the wavelength of 315.109 nm and (b) $y^3P_2^\circ \leftarrow a^3F_3$ transitions with the wavelength of 316.008 nm. The solid lines are the least-squares fits to Eq.(6) that were used to extract photoionization cross sections.

V. ACKNOWLEDGMENTS

This work is supported by the National Natural Science Foundation of China (No.10674002 and No.20973001) and the Science Foundation of Anhui Education Committee (No.ZD2007001-1).

[1] M. J. Seaton, J. Phys. B: At. Mol. Opt. Phys. **20**, 6363 (1987).

DOI:10.1088/1674-0068/22/06/615-620

[2] D. E. Rothe, J. Quant. Spectrosc. Radiat. Transfer. **11**, 355 (1971).
[3] R. V. Ambartzumian, N. P. Furzikov, V. S. Letokhov, and A. A. Puretsky, Appl. Phys. **9**, 335 (1976).
[4] U. Heinzmann, D. Schinkowski, and H. D. Zeman, Appl. Phys. **12**, 113 (1977).
[5] J. M. Preses, Phys. Rev. A **32**, 1264 (1985).
[6] C. E. Burkhardt, J. L. Libbert, J. Xu, and J. J. Leventhal, Phys. Rev. A **38**, 5949 (1988).
[7] B. M. Patterson, T. Takekoshi, and R. J. Knize, Phys. Rev. A **59**, 2508 (1998).
[8] N. Amin, S. Mahmood, M. Saleem, M. A. Kalyar, and M. A. Baig, Eur. Phys. J. D **40**, 331 (2006).
[9] N. Amin, S. Mahmood, M. Anwar-ul-Hag, and M. A. Baig, J. Quant. Spectrosc. Radiat. Transfer. **102**, 269 (2006).
[10] M. Rafiq, M. A. Kalyar, and M. A. Baig, J. Phys. B: At. Mol. Opt. Phys. **41**, 1 (2008).
[11] N. Amin, S. Mahmood, S. U. Haq, M. A. Kalyar, M. Rafiq, and M. A. Baig, J. Quant. Spectrosc. Radiat. Transfer. **109**, 863 (2008).
[12] L. W. He, C. E. Burkhardt, M. Ciocca, and J. J. Leventhal, Phys. Rev. Lett. **67**, 2131 (1991).
[13] B. Willke and M. Kock, Phys. Rev. A **43**, 6433 (1991).
[14] M. Rafiq, S. Hussain, M. Saleem, M. A. Kalyar, and M. A. Baig, J. Phys. B: At. Mol. Opt. Phys. **40**, 2291 (2007).
[15] E. B. Saloman, Spectrochimica Acta Part B **45**, 37 (1990).
[16] S. Saloman, Spectrochimica Acta Part B **46**, 319 (1991).
[17] E. B. Saloman, Spectrochimica Acta Part B **47**, 517 (1992).
[18] S. Saloman, Spectrochimica Acta Part B **48**, 1139 (1993).
[19] O. Gobert, T. Gibert, B. Dubreuil, P. Gelin, and J. L. Debrun, J. Appl. Phys. **70**, 7602 (1991).
[20] R. Cong, Y. Cheng, J. Yang, J. Fan, G. Yao, X. Ji, X. Zheng, and Z. Cui, J. Appl. Phys. **106**, 013103 (2009).
[21] T. Wang, X. Zheng, C. Li, and Y. Chen, Chem. Phys. Lett. **425**, 185 (2006).
[22] X. F. Zheng, T. T. Wang, C. Y. Li, Y. Chen, and J. S. Zhang, Chin. J. Chem. Phys. **20**, 372 (2007).
[23] F. B. Dunning and R. F. Stebbings, Phys. Rev. Lett. **32**, 1286 (1974).
[24] M. B. Das, D. Mitra, and S. Karmakar, Physica Scripta **71**, 599 (2005).
[25] J. S. Coursey, D. J. Schwab, and R. A. Dragoset, *in Atomic Weights and Isotopic Compositions* (*version* 2.4.1), Gaithersburg, MD: National Institute of Standards and Technology, (2005).
[26] P. Forsberg, Physica Scripta **44**, 446 (1991).
[27] Y. Ralchenko, A. E. Kramida, and J. Reader, *in NIST Atomic Spectra Database* (*version* 3.1.5), Gaithersburg, MD: National Institute of Standards and Technology, (2008).

DOI:10.1088/1674-0068/22/06/615-620